Published in final edited form as:

Oncogene. 2009 July 16; 28(28): 2556–2568. doi:10.1038/onc.2009.118.

A Novel Role for MAP1 LC3 in Non-Autophagic Cytoplasmic Vacuolation Death of Cancer Cells

Rekha Kar, **Prajjal K Singha**, **Manjeri A Venkatachalam**, and **Pothana Saikumar***

Department of Pathology, University of Texas Health Science Center at San Antonio, San Antonio, TX 78229

Abstract

Thiol reactive cyclopentenone prostaglandin, 15-deoxy-$\Delta^{12, 14}$-Prostaglandin J_2, induced a novel, non-apoptotic and Map1 LC3 dependent but non-autophagic form of cell death in colon, breast and prostate cancer cell lines, characterized by extensive cytoplasmic vacuolation with dilatation of endoplasmic reticulum. Disruption of sulfhydryl homeostasis, which resulted in ER stress, accumulation of ubiquitinated proteins and subsequent ER dilation, contributed to PPARγ independent cell death by 15d-PGJ2. Absence of intracellular organelles in these vacuoles, shown by Electron Microscopy and unique fragmentation of Lamin B, suggested this form of cell death to be different from autophagy and apoptosis. Cell death induced by 15d-PGJ2 is prevented by cycloheximide and actinomycin D, suggesting a requirement of new protein synthesis for death with cytoplasmic vacuolation. Here, we report for the first time that upregulation and processing of autophagy marker LC3 is an important event in non-autophagic cytoplasmic vacuolation and cell death. Notably, knockdown of LC3 conferred significant protection against 15d-PGJ2 induced cytoplasmic vacuolation and cell death suggesting a novel role of LC3 in a death process other than autophagy.

Keywords

Cell Death; Cytoplasmic Vacuolation; LC3; ER stress; MAPK; 15d-PGJ2

Introduction

Irradiation and chemotherapeutic drugs kill cancer cells typically through induction of apoptosis. However, most cancer cells show resistance to chemotherapy because of genetic mutations or deletions in the pro-apoptotic molecules like Bax and/or overexpression of anti-apoptotic molecules like Bcl2 or XIAP (Kaufmann and Vaux 2003, Longley and Johnston 2005, Reed 1999). Therefore, to achieve more efficient cancer therapeutic effects, it is important to find alternative approaches to induce non-apoptotic cell death, which has been shown to play an important role in physiological processes (Lockshin and Zakeri 2004)

*Address correspondence to: Pothana Saikumar, PhD; Department of Pathology, University of Texas health Science Center at San Antonio, 7703 Floyd Curl Drive, San Antonio, TX 78229. E-mail: saikumar@uthscsa.edu, Telephone: 210-567-6597, Fax: 210-567-2367.

and pathological conditions (Proskuryakov et al 2003). Furthermore, non-apoptotic cell death has often been detected in cells that are resistant to apoptosis (Naito et al 2004, Roninson et al 2001).

Several forms of non-apoptotic cell death such as autophagy, mitotic catastrophe, necrosis, and paraptosis have been described (Broker et al 2005). While apoptosis is characterized by cellular and nuclear fragmentation through caspase activation (Nicholson and Thornberry 1997, Porter et al 1997), non-apoptotic programmed cell death occurs in two major forms namely, autophagy, involving sequestration of cytoplasm and organelles within double membrane structures and their eventual degradation by lysosomal hydrolases (Huang and Klionsky 2002, Noda et al 2002, Ohsumi 2001) and paraptosis, associated with extensive cytoplasmic vacuolation, swelling of ER and mitochondria, absence of caspase activation and nuclear changes (Sperandio et al 2000). Though the molecular mechanisms of cell death and the basic components involved in apoptosis and autophagy are well characterized, much less is known regarding the mechanisms involved in cell death by paraptosis or cytoplasmic vacuolation.

Cyclopentenone prostaglandin derivatives that arise from free radical-induced peroxidation of arachidonic acid have gained interest in their anti-inflammatory, antiviral and antiproliferative properties. The prostaglandin derivative 15-deoxy-$\Delta^{12,14}$-PGJ2 (15d-PGJ2), an endogenous ligand of peroxisome proliferator-activated receptor γ (PPARγ), especially has been found to have potent antiproliferative activities mediated by both PPARγ - dependent and - independent mechanisms (Butler et al 2000, Lin et al 2007, Morosetti et al 2004, Ray et al 2006). The PPARγ independent effects of 15d-PGJ2 were shown to be mediated by either ROS production or covalent modification of proteins via the α, β unsaturated ketone in the cyclopentenone ring of 15d-PGJ2 (Cernuda-Morollon et al 2001, Chen et al 2002, Chen et al 2005, Cho et al 2006, Perez-Sala et al 2003). Although the antiproliferative role of 15d-PGJ2 was shown to be associated with its apoptosis inducing effects in a variety of cell lines including pancreatic beta cells, hepatic myofibroblasts, malignant B cells, breast cancer cells and glioma cells (Chambers et al 2007, Chen et al 2005, Li et al 2001, Morosetti et al 2004), a single report suggested that 15d-PGJ2 could induce non-apoptotic, autophagic death in prostate cancer cells, which was not well characterized (Butler et al 2000).

MAP1 LC3 was originally identified as a protein that co-purifies with large microtubule associated proteins MAP1A and MAP1B from rat brain (Mann and Hammarback 1994). In normal cells, LC3, a homologue of yeast APG8p was shown to exist in two forms, LC3 I (18kDa), a cytosolic form, and LC3 II (16 kDa), the membrane bound shorter form derived from LC3 I by proteolysis and lipid modification (Tanida et al 2001, Tanida et al 2002). During autophagy, LC3 I was shown to be processed into LC3 II before localizing to autophagosomal membranes, suggesting that LC3 processing is a marker of autophagy (Kabeya et al 2000).

Here, we report that the cyclopentenone prostaglandin 15d-PGJ2 induces death associated with vacuolation in HCT116, MDAMB231 and DU145 cancer cells derived from colon, breast and prostate, respectively. Specifically, investigation of the mechanisms by which

cytoplasmic vacuolation develops suggested the dilation of endoplasmic reticulum (ER), ER stress and the involvement of MAP1 LC3B, a protein that has been linked to autophagy. The lack of increased autophagy shown by electron microscopy, and the failure of PI3-Kinase inhibitors to block either the 15d-PGJ2 mediated induction of LC3 or its proteolytic processing suggested that LC3 was involved in a non-autophagic cell death process. Interventions that blocked LC3 induction, either by gene knockdown or chemical inhibitors, dramatically reduced cytoplasmic vacuolation thus illuminating a novel role for LC3 in the ER dilation that results in death by cytoplasmic vacuolation.

Results

15d-PGJ2 induces cytoplasmic vacuolation and cell death in a variety of cancer cells

Treatment with 15d-PGJ2 induced extensive cytoplasmic vacuolation in apoptosis-resistant HCT116 colon cancer cells, MDAMB231 breast cancer cells, and prostate cancer cell line DU145 within 9h (Fig.1A) with no obvious nuclear changes (Fig. 1A and Fig 3A). The death inducing effects of 15d-PGJ2 on cancer cells was determined by both clonogenic survival assay as well as MTT assay. The number of surviving colonies decreased after 15d-PGJ2 treatment in a dose dependent manner in all three cell lines (Fig.1B), suggesting cytotoxic effects of 15d-PGJ2 on cancer cells. Cells that were incubated with 15d-PGJ2 for 9h exhibited cytoplasmic vacuolation and died afterward even if 15d-PGJ2 was absent or continually present (Fig. 1C) suggesting that vacuolation results in irreversible cell injury to cancer cells. Cytoplasmic vacuolation and cell death induced by 15d-PGJ2 was not blocked by PPARγ antagonists GW9662 and T0070907 (Supplemental Fig.1), suggesting involvement of PPARγ independent pathways. Inclusion of z-VAD or q-VD, broad spectrum inhibitors of caspases, prevented neither cytoplasmic vacuolation (Fig. 2A) nor cell death (Fig.2B) in HCT116 cells. Moreover, screening for active caspase-3 in 15d-PGJ2 cells by Western blotting or immunofluorescence gave no signal (data not shown) suggesting that caspases and caspase activation had no role in 15d-PGJ2 induced vacuolation cell death. Similar results were also seen in MDA-MB231 and DU145 (data not shown). In addition, 15d-PGJ2 treated HCT116 colon cancer cells showed random DNA fragmentation that appears as a smear during agarose gel electrophoresis (Fig.2C, lanes 6 and 7). In contrast, 15d-PGJ2 treated, non-transformed but immortalized, rat kidney proximal tubule cells (RPTC) underwent apoptotic cell death and their DNA gave a characteristic ladder like pattern on agarose gels (Fig.2C, lane 2). To further distinguish vacuolation death from apoptosis, we have compared proteolytic degradation of nuclear Lamin B in HCT 116 cells undergoing vacuolation death, in the presence or absence of caspase inhibitor z-VAD, with HeLa cells undergoing apoptotic cell death induced by actinomycin D. Lamin B showed a distinct cleavage pattern in cells dying by vacuolation (Fig. 2D, Lanes 2 and 3) compared to cells dying by apoptosis (Fig. 2D, Lane 5). These results clearly suggested that cytoplasmic vacuolation results in a distinct but novel form of non-apoptotic cell death.

Cytoplasmic vacuoles induced by 15d-PGJ2 are the dilated cisternae of ER

By electron microscopy, 15d-PGJ2 induced vacuoles appeared clear and lacked any visible cytoplasmic material thus ruling out autophagy as the mode of cell death (Fig. 3A).

Furthermore, they appeared to have been derived from fused and swollen ER cisternae that had pushed the cytoplasm and other organelles closer to the nucleus (Fig. 3A). To confirm that 15d-PGJ2 induced vacuoles were derived from ER cisternae; electron micrographs were obtained at a higher resolution and analyzed for rough endoplasmic reticulum (RER). As shown in Fig. 3B, ribosomes were aligned with RER membrane in normal cells. In 15d-PGJ2 treated cells, swollen RER that were shedding ribosomes could be identified (see arrows in Fig. 3B). To further confirm that 15d-PGJ2 induced vacuoles were derived from ER cisternae, cells were immunostained with ER-specific markers Calnexin or Calreticulin, which showed a reticular pattern characteristic of ER in normal cells. Following treatment with 15d-PGJ2, antibodies to ER markers stained numerous cytoplasmic vacuoles (Fig. 3C and supplemental Fig.7).

Upregulation of ER-stress proteins and ubiquitination by 15d-PGJ2

Marked dilation of ER cisternae by 15d-PGJ2 (Fig. 3) suggested that swelling of the ER compartment might occur as a result of ER stress. Examination of ER-stress markers during 15d-PGJ2 treatment indicated ~2 fold upregulation of CHOP and ~3 fold increase in Bip in a dose and time dependent manner (Figure 4A and B ; supplemental Fig.2); in addition there is an increase in ubiquitinated proteins (Figure 4A and B), reflecting the activation of the unfolded protein response (UPR) pathway. Since BiP/GRP78, an ER luminal HSP70 homologue, is often associated with misfolded protein aggregates in the ER (Hurtley et al 1989), we analyzed its distribution in triton soluble and insoluble fractions upon 15d-PGJ2 treatment. In control cells, Bip was detected mostly in the triton soluble fraction (S); however, 15d-PGJ2 treatment resulted in the migration of Bip to Triton insoluble low-speed and high-speed pellet fractions (P1 and P2, Fig.4C). Similarly, CHOP was detected predominantly in the triton-soluble fraction in control cells, whereas 15d-PGJ2 treatment resulted in CHOP translocation to triton-insoluble low-speed pellet fraction (P1), which is consistent with the fact that ER stress causes nuclear translocation of CHOP (Ghribi et al 2001). In contrast, Glyceraldehyde 3-phosphate dehydrogenase (GAPDH), a cytosolic protein was present mostly in triton-soluble fraction (S) both in untreated and treated cells. Since valosin-containing protein (VCP) plays an important role in expelling misfolded proteins from the endoplasmic reticulum (ER) to degrade them in the cytoplasm by the ubiquitin-proteasome system, we compared the relative distribution of VCP in normal and 15d-PGJ2 treated cells. While VCP was predominantly associated with Triton soluble fraction in normal cells (S), 15d-PGJ2 treatment resulted in its migration to triton-insoluble pellet fractions (P1 and P2; Fig. 4C). Similar redistribution of VCP was also reported under velcade induced cytoplasmic vacuolation (Mimnaugh et al 2006).

15d-PGJ2 induced cytoplasmic vacuolation requires new protein synthesis

Cytoplasmic vacuolation induced by 15d-PGJ2 was completely blocked by the inhibitors of transcription and translation, actinomycin D (act D) and cycloheximide (CHX) respectively (Figure 4D), suggesting its similarity with paraptosis described by Sperandio et al, both in terms of vacuolation and its prevention by act D and CHX (Sperandio et al 2000). Inclusion of act D or CHX dramatically reduced ER stress, as shown by the lack of upregulation of ER stress markers Bip and CHOP (supplemental Fig.4), and preserved the viability of 15d-PGJ2 treated cancer cells as shown by complete restoration of their ability to form colonies in a

clonogenic assay (Figure 4E). Increased ubiquitination and aggregation of proteins into Triton insoluble fraction, by 15d-PGJ2, was also prevented by CHX and act D (Fig. 4F). Taken together, it appears that 15d-PGJ2 induces extensive misfolding of newly synthesized proteins forming insoluble aggregates resulting in ER swelling, and that this process depends on transcription and translation of new protein.

Autophagy-independent expression and processing of LC3 induced by 15d-PGJ2

Surprisingly, 15d-PGJ2 induced ~10 fold increase in LC3-I, the cytosolic form of microtubule-associated protein 1 light chain 3 (LC3), and ~15–20 fold increase in its processed membrane-bound form LC3-II in a dose and time dependent manner (Figs. 5A and 5B; Supplemental Fig.3). Since LC3 was shown to be involved in the formation of vacuoles during autophagy, we checked for similarities between autophagy and 15d-PGJ2 induced cytoplasmic vacuolation in terms of LC3 processing. PI3-kinase inhibitors are known to block the autophagy-mediated processing of LC3. Therefore, we tested the sensitivity of cytoplasmic vacuolation mediated LC3 processing to these inhibitors, and compared the LC3 processing that occurs during serum starvation induced autophagy in HeLa cells (Kabeya et al 2000) and 15d-PGJ2 induced cytoplasmic vacuolation in HCT116 cells. Starvation in HeLa cells did not increase the expression of LC3 but only increased processing of LC3-I to LC3-II (Fig.5C, compare lanes 1and 2), which was prevented by all three inhibitors of PI3-kinase (PI3-K), wortmannin (WM), LY294002 (LY) and 3 methyladenine (3MA; Fig.5C). In contrast, increased expression and processing of LC3 in vacuolated HCT116 cells was not blocked by PI3-K inhibitors WM, LY and 3MA (Fig. 5E). Analysis of cytoplasm and membrane fractions of autophagic HeLa cells and vacuolated HCT116 cells clearly indicated that in both, LC3-I was localized to the cytoplasm, while the processed LC3-II was recruited to the membrane bound fraction (Fig.5D and 5F). Thus our results suggested that the mechanisms involved in the induction and processing of LC3 during cytoplasmic vacuolation are distinct from the mechanisms involved in autophagy-induced LC3 processing. Since we do not yet have suitable antibodies for LC3 immunofluorescence, we generated HCT 116 cells that constitutively expressed GFP-LC3. Though we observed increased granulation of GFP-LC3 during starvation induced autophagy, 15d-PGJ2 induced cytoplasmic vacuolation resulted in perivacuolar distribution of GFP-LC3 (Fig. 5G). Since three isoforms of MAP1LC3 exist in human cells, we asked the question which isoforms are being induced during cytoplasmic vacuolation. Interestingly, only MAP1 LC3B but not MAP1 LC3A or MAP1 LC3C was dramatically induced during 15d-PGJ2-mediated cytoplasmic vacuolation (Fig. 5H).

Thiol-antioxidants but not other ROS scavengers block 15d-PGJ2 induced cytoplasmic vacuolation

The anti-neoplastic effects of 15d-PGJ2 were earlier shown to be exerted through ROS production (Chen et al 2002). Therefore, we tested the effect of several antioxidants on 15d-PGJ2 induced vacuolation and cell death in HCT116 cells. To our surprise, ROS scavengers TEMPOL, a Superoxide dismutase mimetic, and Trolox, a vitamin E analog, failed to block 15d-PGJ2 induced cytoplasmic vacuolation and cell death in HCT116 colon cancer cells (Fig. 6A and 6B). In sharp contrast, the thiol antioxidants N-α-Acetyl-L-cysteine (NAC) and N-mercapto-propionyl-glycine (NMPG) prevented 15d-PGJ2 induced cytoplasmic

vacuolation in HCT116 cells (Fig. 6A) and restored their ability to survive and form clones in a clonogenic assay (Fig. 6B). Moreover, these thiol antioxidants, but not TEMPOL and Trolox, also significantly prevented 15d-PGJ2 induced expression of ER stress markers Bip and CHOP (Fig. 6C), and reduced the accumulation of ubiquitinated proteins (Fig. 6D). Furthermore, both NAC and NMPG but not TEMPOL and Trolox blocked 15d-PGJ2 induced expression and processing of LC3 (Fig. 6C). These results indicate that the effects of 15d-PGJ2 are probably mediated through its ability to covalently modify free sulfhydryl groups on proteins and not through ROS production.

Role of MAP kinases in 15d-PGJ2 induced cytoplasmic vacuolation

To elucidate the signaling mechanisms that are involved in regulating 15d-PGJ2 induced cytoplasmic vacuolation; we monitored the activation of MAP kinases by immunoblotting with phosphospecific antibodies. Treatment with 15d-PGJ2 resulted in the predominant activation of MAP kinase, ERK (extracellular signal-regulated kinase), and marginal activation of two other MAP kinases, SAPK/JNK and p38 (Figure 7A). However, only inhibitors of ERK pathway, U0126 and MEK inhibitor I but not the inactive analog U0124, showed significant reduction in the number of vacuolated cells (Fig.7C), whereas inhibitors of p38 (SB203580) and SAPK (SP600125) had no effect (Fig. 7C). Interestingly, ERK inhibitors also decreased 15d-PGJ2 induced expression and processing of LC3 (Fig.7B, lanes 4 and 8), while p38 and SAPK inhibitors had no effect (Fig. 7B, lanes 12, 14 and 16).

Loss of lysosomal protease activity is not responsible for LC3 induction

To find out whether expression of LC3 is related to decreased lysosomal function by 15d-PGJ2, we analyzed the effect of 15d-PGJ2, leupeptin, q-VD on Cathepsin B and L, lysosomal endopeptidases. Leupeptin completely blocked lysosomal cathepsin activity when it was added to either cell extracts (Fig. 8A) or intact cells (Fig. 8B), but caused only a slight increase in LC3 protein levels in the intact cells (Fig. 8C, lane 4). In contrast, 15d-PGJ2 did not affect cathepsin activity when it was added directly to cell extracts (Fig. 8A), caused only a ~50% decrease of cathepsin activity when it was added to intact cells (Fig. 8B), but caused large increases of LC3 protein in the intact cells (Fig. 8C, lane 2) suggesting that lysosomal inhibition did not effect LC3 induction. In fact, blockage of 15d-PGJ2 induced LC3 expression by transcription and translational inhibitors (supplemental Fig. 4) and MAPK inhibitors suggest alternative novel mechanisms to be responsible for LC3 upregulation.

Map1 LC3B knockdown conferred protection against 15d-PGJ2 induced cytoplasmic vacuolation and cell death

A dose and time dependent increase in the expression and processing of LC3 by 15d-PGJ2, and prevention of LC3 induction and processing by reagents that blocked cytoplasmic vacuolation suggested that LC3 may play an important role in cytoplasmic vacuolation death. To test the role played by LC3 in cytoplasmic vacuolation, LC3 expression was blocked by gene knockdown techniques using shRNA. Initially, three different shRNA sequences were screened to knockdown LC3 expression by transient transfection and one sequence was found to be more effective than others in reducing LC3 expression and cytoplasmic vacuolation (not shown). We used this construct for stably expressing MAP1

LC3B-shRNA in HCT116 cells. A GFP-shRNA construct was used as a control. Knockdown of LC3 (Fig. 9A) conferred significant protection against 15d-PGJ2 induced cytoplasmic vacuolation as revealed by phase contrast microscopy (Figs. 9B and 9C). Although 15d-PGJ2 treated LC3 knockdown cells showed only moderate decreases of Bip expression and ubiquitinated protein accumulation, CHOP induction was significantly blocked (Fig. 9A). Furthermore, cell viability assays revealed that knockdown of LC3 significantly protected HCT116 cells from 15d-PGJ2 induced cell death (Fig. 9D). Decreased expression of LC3 also resulted in slower growth rate of HCT116 cells, which was consistent with increased expression of p21, p27 and p53 proteins (Fig. 9E).

Discussion

This study sheds light on the mechanism of death by cytoplasmic vacuolation induced by 15d-PGJ2 in the cancer cell lines HCT116, DU145 and MDAMB231. The results clearly demonstrated that 15d-PGJ2 induces caspase independent cell death characterized by extensive cytoplasmic vacuolation in apoptosis resistant cancer cell lines. This form of death was associated with ER stress and required new protein synthesis (Fig. 4). 15d-PGJ2 resulted in massive increases of ubiquitinated proteins and their aggregation as evidenced by their detection in the triton insoluble fractions (Fig. 4). Based on our results, it appears that disruption of sulfhydryl homeostasis might be the critical factor in this form of cell death as only thiol antioxidants, NAC and NMPG, but not other ROS scavengers TEMPOL and Trolox, prevented the accumulation of ubiquitinated proteins, induction of ER stress markers, and cytoplasmic vacuolation (Fig. 6).

The present study also shows for the first time that 15d-PGJ2 induced non-autophagic cell death was associated with induction and processing of the autophagy marker MAP1 LC3B (Fig. 5). Unlike autophagy, where all three isoforms of LC3 seems to mark the autophagic vacuoles (He et al 2003), cytoplasmic vacuolation likely requires only LC3B isoform (Fig. 5H). However, the LC3 processing that occurred during cytoplasmic vacuolation was shown to be quite distinct from autophagy mediated processing of LC3. Both class I and Class III PI3-kinase inhibitors, which blocked autophagic processing of LC3, failed to prevent 15d-PGJ2-mediated induction and conversion of LC3 (Fig. 5). The exact role of LC3 in 15d-PGJ2 induced ER membrane fusion and formation of cytoplasmic vacuoles still remains to be determined. Notably, all agents that blocked cytoplasmic vacuolation — NAC, NMPG, Act D, CHX, U0126 and MEK inhibitor I — inhibited both the induction and processing of LC3 (Fig. 6, Fig 7 and supplemental Fig. 4). Additionally, the protection offered by LC3 knockdown clearly points to its critical role in cytoplasmic vacuolation death induced by 15d-PGJ2 (Fig. 9). Activation of MAPK signaling by 15d-PGJ2 has been reported in various cell types (Hashimoto et al 2004, Kimura et al 2008). In the present study, activation of subfamilies MAPK were noted (Fig. 7). Specific inhibitors of ERK significantly prevented 15d-PGJ2-induced cytoplasmic vacuolation as well as LC3 induction and processing, indicating the involvement of MAPK pathways.

Accumulation of misfolded proteins invariably results in the activation of several intracellular signaling pathways that include the unfolded protein response (UPR) and ER-associated degradation (ERAD) to protect cells from proteotoxicity. Therefore, enhanced

rates of accumulation of misfolded proteins increase the dependency of cells on optimal proteasomal function. However, failure of the proteasomal machinery would lead to further accumulation of misfolded proteins in the ER and cytoplasm making them toxic to the cells. In this regard, proteasome inhibitors appear to be attractive anti-neoplastic therapeutic drugs. Overwhelming of cells by misfolded proteins often results in the failure of UPR and ERAD, the ER quality control machineries, to remove these unwanted toxic proteins and thus may lead to cell death. Indeed, cancer cells are much more sensitive to the death effects of proteasome inhibition than normal cells (Nawrocki et al 2005).

Since 15d-PGJ2 induced cytoplasmic vacuolation was indeed due to ER dysfunction, this form of cell death warrants further attention in the treatment of cancer. In this regard, drugs that simulate the actions of 15d-PGJ2 may be more suitable as anti-neoplastic agent as they could have the potential to covalently modify sulfhydryl groups causing protein misfolding as well as inhibit the proteasomal degradation machinery (Ishii et al 2005, Wang et al 2006). Newly synthesized proteins with exposed sulfhydryls are likely to be more sensitive than mature proteins for covalent modification by 15d-PGJ2 analogs. Because of their absolute requirement for new protein synthesis, rapidly growing cancer cells would be more susceptible than quiescent normal cells to 15d-PGJ2 induced cell death. It is noteworthy that cycloheximide and actinomycin D, drugs that block new protein synthesis, protected cancer cells from 15d-PGJ2 induced cytoplasmic vacuolation death by reducing the overall load of misfolded proteins on the endoplasmic reticulum. It is interesting to note that the slower growth rate of LC3 knockdown cells may also contribute to a decreased rate of misfolded protein formation, thus reducing the subsequent load on ER. Interestingly, other cyclopentenone prostaglandins like PGA1 and PGA2 were less potent than 15d-PGJ2 in inducing cytoplasmic vacuolation, ER stress or LC3 expression (supplemental Fig.5), thus suggesting uniqueness of 15d-PGJ2 in mediating non-autophagic and non-apoptotic cell death. Recently, it was found that autophagy accelerates the degradation of p62 protein, also called sequestosome 1 (SQSTM1), which is known to associate with ubiquitinated proteins (Bjorkoy et al 2005, Pursiheimo et al 2009). It has been reported that there is a good correlation between inhibition of autophagy and increased levels of p62 (Bjorkoy et al 2005, Pankiv et al 2007). Interestingly, our results show that 15d-PGJ2 treatment causes increased levels of p62 suggesting that autophagy may be inhibited in vacuolated cells (Supplemental Fig. 6), which is further supported by the inhibition of lysosomal cathepsin activity by 15d-PGJ2 (Fig. 8) .

Overall, the above studies highlight the importance of drug induced cytoplasmic vacuolation as an alternative form of programmed cell death, which can be further exploited to treat apoptosis resistant tumors.

Materials and Methods

Materials

HCT116 cells (a kind gift from Dr. Bert Vogelstein) were grown in Mc COY's 5A supplemented with FBS and Penicillin-Streptomycin. HeLa, DU145 and MDAMB231 cells were from ATCC (Manassas, VA) and were grown according to recommendations from ATCC. The compounds SB203580, SP600125, MEK inhibitor I, U0126, U0124, N-α-

Acetyl-L-cysteine (NAC), TEMPOL and Trolox were purchased from Calbiochem (San diego, CA). 15-deoxy-$\Delta^{12,14}$-Prostaglandin J_2, prostaglandins A1, A2 and D2, GW9662 and T0070907 were from Cayman chemicals (Ann Arbor, MI). Actinomycin D, cycloheximide, N-mercapto-propionyl-glycine (NMPG), LY294002, Wortmannin and 3-Methyadenine were obtained from Sigma, (St Louis, MO), zVAD and qVD from MP Biomedicals (Aurora, OH). Bip rat monoclonal and Chop and Lamin B rabbit polyclonals, p53 mouse monoclonal antibodies were from Santa Cruz Biotechnology (Santa Cruz, CA). The p21 mouse monoclonal antibody was from Upstate biotechnology (Lake Placid, NY). P27 antibody was from Lab vision (Fremont, CA). Ubiquitin antibody was from Biomol (Plymouth Meeting, PA) and VCP antibody was from Affinity Bioreagents (Golden, CO). Antibodies to phospho-p38, phospho-SAPK, phospho-ERK were from Cell signaling Technology (Danvers, MA). Calreticulin rabbit polyclonal was a kind gift from Dr. Robert A. Clark, UTHSCSA. LC3 antibody and GFP-LC3 constructs were kind gifts from Dr. Tamotsu Yoshimori, Osaka university (Japan). MAP1 LC3B antibody was also obtained from Cell Signaling (Danvers, MA). Horseradish peroxidase-conjugated and preadsorbed secondary antibodies to mouse and rabbit were obtained from Jackson Immunoresearch Laboratories (Westgrove, PA). All other reagents were of the highest grade available.

15d-PGJ2 treatment and Cell Viability

Cells were plated at ~0.11×10^6 cells/cm^2 with suitable growth medium in 35mm dishes or multiwell plates. After overnight growth, cells were incubated with indicated concentrations of 15d-PGJ2 in fresh complete growth medium for indicated times. Control and experimental cells after 9h of treatment with 15d-PGJ2 at concentrations indicated as well as in combination with different inhibitors, were either trypsinized for Clonogenic survival assay, a method of choice to determine cell reproductive death after treatment with cytotoxic agents. Cell viability was also determined by 3-(4,5-dimethylthiazol-2-yl)-2,5-diphenyltetrazolium bromide (MTT) assay (Mosmann 1983) after 9h or 24, 48 and 72 h incubation of cells with 15d-PGJ2. For each data point, triplicate cultures were prepared and data represents average of at least three independent experiments.

Autophagy

To induce autophagy, HeLa or HCT116 cells were starved in Hanks' balanced salt solution (HBSS) for 1h at 37°C with or without the inhibitors of autophagy, wortmannin (WM, 0.1, 0.5 and 1μM), LY294002 (LY, 50 and 100μM) and 3-methyladenine (3-MA, 10mM), after which cells were lysed in 2x laemmli buffer and were subjected to immunoanalysis using anti-LC3 antibody.

Cathepsin assay

Cytosolic fraction and membrane fraction that contain organelle bound proteins including lysosomal enzymes were prepared as described before (Saikumar et al 1998). To measure Cathepsin B and L activity, 25 μg of membrane lysates were added to reaction mixtures containing 50 μM peptide substrate (z-Phe-Arg-AMC), 100 mM HEPES, 10% sucrose, 0.1% CHAPS, 1 mM EDTA, and 10 mM DTT pH 7.4 in a total volume of 200 μl and incubated at 37°C for 1 h. Production of 7-amino-4-methylcoumarin (AMC) was monitored in an

SpectroFluor plate reader (Tecan US Inc., Research Triangle Park, NC, USA) using excitation wavelength 360 nm and emission wavelength 460 nm.

DNA Laddering

DNA fragmentation was analyzed as described previously (Saikumar et al 1998). Control and experimental cells were lysed in hypotonic buffer (10 mM Tris, 2 mM EDTA, pH 7.4) containing 0.5% Triton X-100. The resultant supernatant was treated with proteinase K and RNase A, extracted with phenol:chloroform and ethanol precipitated. DNA precipitates were dissolved in 10 mM Tris, 1 mM EDTA at pH 8.0 and analyzed by 1.5% agarose gel electrophoresis.

Electron microscopy

Control and experimental cells in a 35 mm dish were fixed with 2.5% glutaraldehyde in 0.1 M sodium cacolylate buffer and were then incubated with osmium tetroxide (OsO4) at 4°C for 1h. The cells were then incubated overnight in 1% uranyl acetate at 4°C after which they were further processed at the Electron Microscopy Core Facility in the Department of Pathology, UTHSCSA.

Immunocytochemistry

Control and 15d-PGJ2 treated experimental cells were fixed with 4% paraformaldehyde in phosphate buffered saline and then were exposed to primary antibody, anti-calnexin or anti calreticulin followed by CY3-conjugated anti rabbit or anti-mouse secondary antibodies. Coverslips were mounted with prolonged antifade mounting media (Invitrogen) with or without DAPI and cells were visualized in Olympus FV-500 laser scanning confocal fluorescent microscope.

Subcellular Fractionation

Cytosolic and membrane fractions were prepared as described before (Saikumar et al 1998). To obtain detergent soluble and insoluble fractions, control and experimental cells were lysed in dishes with the lysis buffer containing 1% Triton X-100 in isotonic buffer A containing protease inhibitors, scraped, collected into centrifuge tubes and incubated over ice for 30min. The lysates were centrifuged for 20min at 1,500×g in 4°C to obtain pellet P1 and the resulting supernatant was further centrifuged at 100,000×g for 1h to obtain pellet P2 and supernatant S. The pellets P1 and P2 were dissolved in 2x laemmli buffer.

Immunoanalysis

All proteins from different cell lysates were resolved by SDS-PAGE in Xcell II mini cell on 10% or 4–12% (gradient) NuPAGE gels (Invitrogen, CA) with MOPS or MES running buffer, then were electroblotted onto PVDF membranes (0.2 μm) using manufacturer's directions. Western blotting using appropriate primary antibodies and peroxidase-conjugated suitable secondary antibodies was performed on the above membranes. Chemiluminescent substrates from Pierce (Rockford, IL) were used to detect antigen-antibody complexes on the PVDF membrane. Densitometry was done on immunoblots using Alpha Imager apparatus (Alpha Innotech, CA) equipped with alpha view software.

Quantitative real time-PCR for LC3 expression

To identify which of MAP1LC3isoforms are upregulated by 15d-PGJ2 treatment, we used quantitative real time-PCR (q-PCR). Total RNA from HCT116 cells treated with 15d-PGJ2 for 0, 2, 6 or 9 hr was isolated using RNAeasy kit according to the manufacturer's instructions (Qiagen). One microgram of total RNA was reverse-transcribed in 50 μl at 48 °C for 2 h using High Capacity cDNA Archive Kit from Applied Biosystems. Amplification of cDNA was carried out using the following primers and SYBR green PCR master mix in an Applied Biosystems 7500 Real-Time PCR System. The primers used for amplification are: MAP1 LC3A Forward primer (CGTCCTGGACAAGACCAAGT) and Reverse primer (CTCGTCTTTCTCCTGCTCGT); MAP1 LC3B Forward primer (AGCAGCATCCAACCAAAATC), and Reverse primer (CTGTGTCCGTTCACCAACAG); MAP1 LC3C Forward primer (CGGAAGCCTTTTACTTGCTG) and Reverse primer (GTCTGTCCTCAAGGCTGCTC). The threshold cycle (C_t) values, as defined by the default setting, were measured by an ABI Prism 7500 Sequence Detection System. 18srRNA was used as an internal control. Triplicate samples were measured and averaged.

LC3 Knockdown

To stably knock down endogenous LC3 expression by RNAi, the short-hairpin RNA expression cassettes generated by annealing 64-nucleotide sequences containing the 19-nucleotide sequence from the target transcripts were cloned into pSUPER vector driven by the human H1 promoter. The 19-nucleotide sequence was designed from the following region of human LC3B (bases 418–436). Vector containing short-hairpin sequence for GFP was used as a control. All constructs were verified by DNA sequencing.

Supplementary Material

Refer to Web version on PubMed Central for supplementary material.

Acknowledgements

We thank Dr. Tamotsu Yoshimori of Osaka University, Japan for LC3 antibody and GFP-LC3 construct and Drs. Anthony J. Valente and Robert A. Clark of UTHSCSA, TX for Calreticulin antibody. This work was supported by National Institutes of Health grant DK54472 and Morrison Trust Grant to P.S and National Institutes of Health grant DK37139 to M.A.V.

References

Bjorkoy G, Lamark T, Brech A, Outzen H, Perander M, Overvatn A, et al. p62/SQSTM1 forms protein aggregates degraded by autophagy and has a protective effect on huntingtin-induced cell death. J Cell Biol. 2005; 171:603–614. [PubMed: 16286508]

Broker LE, Kruyt FA, Giaccone G. Cell death independent of caspases: a review. Clin Cancer Res. 2005; 11:3155–3162. [PubMed: 15867207]

Butler R, Mitchell SH, Tindall DJ, Young CY. Nonapoptotic cell death associated with S-phase arrest of prostate cancer cells via the peroxisome proliferator-activated receptor gamma ligand, 15-deoxy-delta12,14-prostaglandin J2. Cell Growth Differ. 2000; 11:49–61. [PubMed: 10672903]

Cernuda-Morollon E, Pineda-Molina E, Canada FJ, Perez-Sala D. 15-Deoxy-Delta 12,14-prostaglandin J2 inhibition of NF-kappaB-DNA binding through covalent modification of the p50 subunit. J Biol Chem. 2001; 276:35530–35536. [PubMed: 11466314]

Chambers KT, Weber SM, Corbett JA. PGJ2-stimulated beta-cell apoptosis is associated with prolonged UPR activation. Am J Physiol Endocrinol Metab. 2007; 292:E1052–E1061. [PubMed: 17148750]

Chen SY, Lu FJ, Gau RJ, Yang ML, Huang TS. 15-Deoxy-delta12,14-prostaglandin J2 induces apoptosis of a thyroid papillary cancer cell line (CG3 cells) through increasing intracellular iron and oxidative stress. Anticancer Drugs. 2002; 13:759–765. [PubMed: 12187333]

Chen YC, Shen SC, Tsai SH. Prostaglandin D(2) and J(2) induce apoptosis in human leukemia cells via activation of the caspase 3 cascade and production of reactive oxygen species. Biochim Biophys Acta. 2005; 1743:291–304. [PubMed: 15843042]

Cho WH, Choi CH, Park JY, Kang SK, Kim YK. 15-deoxy-(Delta12,14)-prostaglandin J2 (15d-PGJ2) induces cell death through caspase-independent mechanism in A172 human glioma cells. Neurochem Res. 2006; 31:1247–1254. [PubMed: 17006759]

Ghribi O, Herman MM, DeWitt DA, Forbes MS, Savory J. Abeta(1–42) and aluminum induce stress in the endoplasmic reticulum in rabbit hippocampus, involving nuclear translocation of gadd 153 and NF-kappaB. Brain Res Mol Brain Res. 2001; 96:30–38. [PubMed: 11731006]

Hashimoto K, Farrow BJ, Evers BM. Activation and role of MAP kinases in 15d-PGJ2-induced apoptosis in the human pancreatic cancer cell line MIA PaCa-2. Pancreas. 2004; 28:153–159. [PubMed: 15028947]

He H, Dang Y, Dai F, Guo Z, Wu J, She X, et al. Post-translational modifications of three members of the human MAP1LC3 family and detection of a novel type of modification for MAP1LC3B. J Biol Chem. 2003; 278:29278–29287. [PubMed: 12740394]

Huang WP, Klionsky DJ. Autophagy in yeast: a review of the molecular machinery. Cell Struct Funct. 2002; 27:409–420. [PubMed: 12576634]

Hurtley SM, Bole DG, Hoover-Litty H, Helenius A, Copeland CS. Interactions of misfolded influenza virus hemagglutinin with binding protein (BiP). J Cell Biol. 1989; 108:2117–2126. [PubMed: 2738090]

Ishii T, Sakurai T, Usami H, Uchida K. Oxidative modification of proteasome: identification of an oxidation-sensitive subunit in 26 S proteasome. Biochemistry. 2005; 44:13893–13901. [PubMed: 16229478]

Kabeya Y, Mizushima N, Ueno T, Yamamoto A, Kirisako T, Noda T, et al. LC3, a mammalian homologue of yeast Apg8p, is localized in autophagosome membranes after processing. Embo J. 2000; 19:5720–5728. [PubMed: 11060023]

Kaufmann SH, Vaux DL. Alterations in the apoptotic machinery and their potential role in anticancer drug resistance. Oncogene. 2003; 22:7414–7430. [PubMed: 14576849]

Kimura H, Li X, Torii K, Okada T, Takahashi N, Fujii H, et al. A natural PPAR-{gamma} agonist, 15-deoxy-delta 12,14-prostaglandin J2, may act as an enhancer of PAI-1 in human proximal renal tubular cells under hypoxic and inflammatory conditions. Nephrol Dial Transplant. 2008

Li L, Tao J, Davaille J, Feral C, Mallat A, Rieusset J, et al. 15-deoxy-Delta 12,14-prostaglandin J2 induces apoptosis of human hepatic myofibroblasts. A pathway involving oxidative stress independently of peroxisome-proliferator-activated receptors. J Biol Chem. 2001; 276:38152–38158. [PubMed: 11477100]

Lin MS, Chen WC, Bai X, Wang YD. Activation of peroxisome proliferator-activated receptor gamma inhibits cell growth via apoptosis and arrest of the cell cycle in human colorectal cancer. J Dig Dis. 2007; 8:82–88. [PubMed: 17532820]

Lockshin RA, Zakeri Z. Caspase-independent cell death? Oncogene. 2004; 23:2766–2773. [PubMed: 15077140]

Longley DB, Johnston PG. Molecular mechanisms of drug resistance. J Pathol. 2005; 205:275–292. [PubMed: 15641020]

Mann SS, Hammarback JA. Molecular characterization of light chain 3. A microtubule binding subunit of MAP1A and MAP1B. J Biol Chem. 1994; 269:11492–11497. [PubMed: 7908909]

Mimnaugh EG, Xu W, Vos M, Yuan X, Neckers L. Endoplasmic reticulum vacuolization and valosin-containing protein relocalization result from simultaneous hsp90 inhibition by geldanamycin and proteasome inhibition by velcade. Mol Cancer Res. 2006; 4:667–681. [PubMed: 16966435]

Morosetti R, Servidei T, Mirabella M, Rutella S, Mangiola A, Maira G, et al. The PPARgamma ligands PGJ2 and rosiglitazone show a differential ability to inhibit proliferation and to induce apoptosis and differentiation of human glioblastoma cell lines. Int J Oncol. 2004; 25:493–502. [PubMed: 15254749]

Mosmann T. Rapid colorimetric assay for cellular growth and survival: application to proliferation and cytotoxicity assays. J Immunol Methods. 1983; 65:55–63. [PubMed: 6606682]

Naito M, Hashimoto C, Masui S, Tsuruo T. Caspase-independent necrotic cell death induced by a radiosensitizer, 8-nitrocaffeine. Cancer Sci. 2004; 95:361–366. [PubMed: 15072596]

Nawrocki ST, Carew JS, Pino MS, Highshaw RA, Dunner K Jr, Huang P, et al. Bortezomib sensitizes pancreatic cancer cells to endoplasmic reticulum stress-mediated apoptosis. Cancer Res. 2005; 65:11658–11666. [PubMed: 16357177]

Nicholson DW, Thornberry NA. Caspases: killer proteases. Trends Biochem Sci. 1997; 22:299–306. [PubMed: 9270303]

Noda T, Suzuki K, Ohsumi Y. Yeast autophagosomes: de novo formation of a membrane structure. Trends Cell Biol. 2002; 12:231–235. [PubMed: 12062171]

Ohsumi Y. Molecular dissection of autophagy: two ubiquitin-like systems. Nat Rev Mol Cell Biol. 2001; 2:211–216. [PubMed: 11265251]

Pankiv S, Clausen TH, Lamark T, Brech A, Bruun JA, Outzen H, et al. p62/SQSTM1 binds directly to Atg8/LC3 to facilitate degradation of ubiquitinated protein aggregates by autophagy. J Biol Chem. 2007; 282:24131–24145. [PubMed: 17580304]

Perez-Sala D, Cernuda-Morollon E, Canada FJ. Molecular basis for the direct inhibition of AP-1 DNA binding by 15-deoxy-Delta 12,14-prostaglandin J2. J Biol Chem. 2003; 278:51251–51260. [PubMed: 14532268]

Porter AG, Ng P, Janicke RU. Death substrates come alive. Bioessays. 1997; 19:501–507. [PubMed: 9204767]

Proskuryakov SY, Konoplyannikov AG, Gabai VL. Necrosis: a specific form of programmed cell death? Exp Cell Res. 2003; 283:1–16. [PubMed: 12565815]

Pursiheimo JP, Rantanen K, Heikkinen PT, Johansen T, Jaakkola PM. Hypoxia-activated autophagy accelerates degradation of SQSTM1/p62. Oncogene. 2009; 28:334–344. [PubMed: 18931699]

Ray DM, Akbiyik F, Phipps RP. The peroxisome proliferator-activated receptor gamma (PPARgamma) ligands 15-deoxy-Delta12,14-prostaglandin J2 and ciglitazone induce human B lymphocyte and B cell lymphoma apoptosis by PPARgamma-independent mechanisms. J Immunol. 2006; 177:5068–5076. [PubMed: 17015690]

Reed JC. Dysregulation of apoptosis in cancer. J Clin Oncol. 1999; 17:2941–2953. [PubMed: 10561374]

Roninson IB, Broude EV, Chang BD. If not apoptosis, then what? Treatment-induced senescence and mitotic catastrophe in tumor cells. Drug Resist Updat. 2001; 4:303–313. [PubMed: 11991684]

Saikumar P, Dong Z, Weinberg JM, Venkatachalam MA. Mechanisms of cell death in hypoxia/reoxygenation injury. Oncogene. 1998; 17:3341–3349. [PubMed: 9916996]

Sperandio S, de Belle I, Bredesen DE. An alternative, nonapoptotic form of programmed cell death. Proc Natl Acad Sci U S A. 2000; 97:14376–14381. [PubMed: 11121041]

Tanida I, Tanida-Miyake E, Ueno T, Kominami E. The human homolog of Saccharomyces cerevisiae Apg7p is a Protein-activating enzyme for multiple substrates including human Apg12p, GATE-16, GABARAP, and MAP-LC3. J Biol Chem. 2001; 276:1701–1706. [PubMed: 11096062]

Tanida I, Tanida-Miyake E, Komatsu M, Ueno T, Kominami E. Human Apg3p/Aut1p homologue is an authentic E2 enzyme for multiple substrates, GATE-16, GABARAP, and MAP-LC3, and facilitates the conjugation of hApg12p to hApg5p. J Biol Chem. 2002; 277:13739–13744. [PubMed: 11825910]

Wang Z, Aris VM, Ogburn KD, Soteropoulos P, Figueiredo-Pereira ME. Prostaglandin J2 alters pro-survival and pro-death gene expression patterns and 26 S proteasome assembly in human neuroblastoma cells. J Biol Chem. 2006; 281:21377–21386. [PubMed: 16737963]

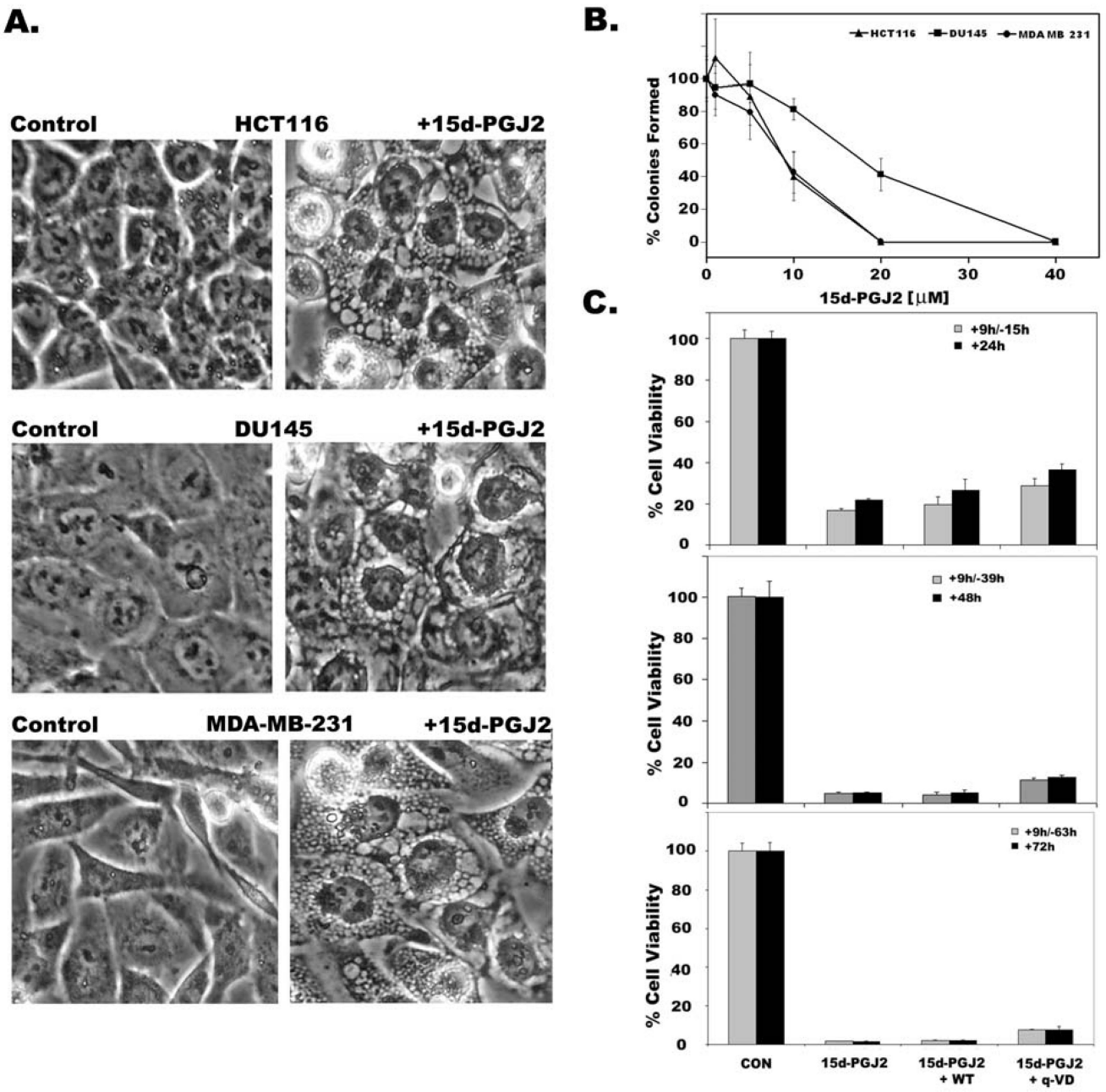

Figure 1. 15d-PGJ2 induces cytoplasmic vacuolation and cell death in cancer cells

HCT116 colon cancer cells, MDAMB231 breast cancer cells, and DU145 prostate cancer cells were treated with 20μM of 15d-PGJ2 for 9h. A. Phase contrast images showing cytoplasmic vacuolation in 15d-PGJ2 treated cells (right panels). Untreated cells were shown in the left panels. B. Death inducing effects of 15d-PGJ2 on HCT116, MDAMB231 and DU145 cancer cells was determined by clonogenic survival after 9h treatment as described in Experimental section. Data represents average of three independent experiments with standard error. C. Decreased cell viability of HCT116 cells as assessed by MTT assay with either continuous presence of drug for 24h, 48h and 72h or treated with

drug for 9h and shifted to normal medium for remaining periods (+9h/−15h, +9h/−39h, +9h/−63h). Effect of autophagy inhibitor Wortmannin (WM) or apoptosis inhibitor (q-VD) on cell viability was also tested. Data represents average of 3 independent experiments ± S.D.

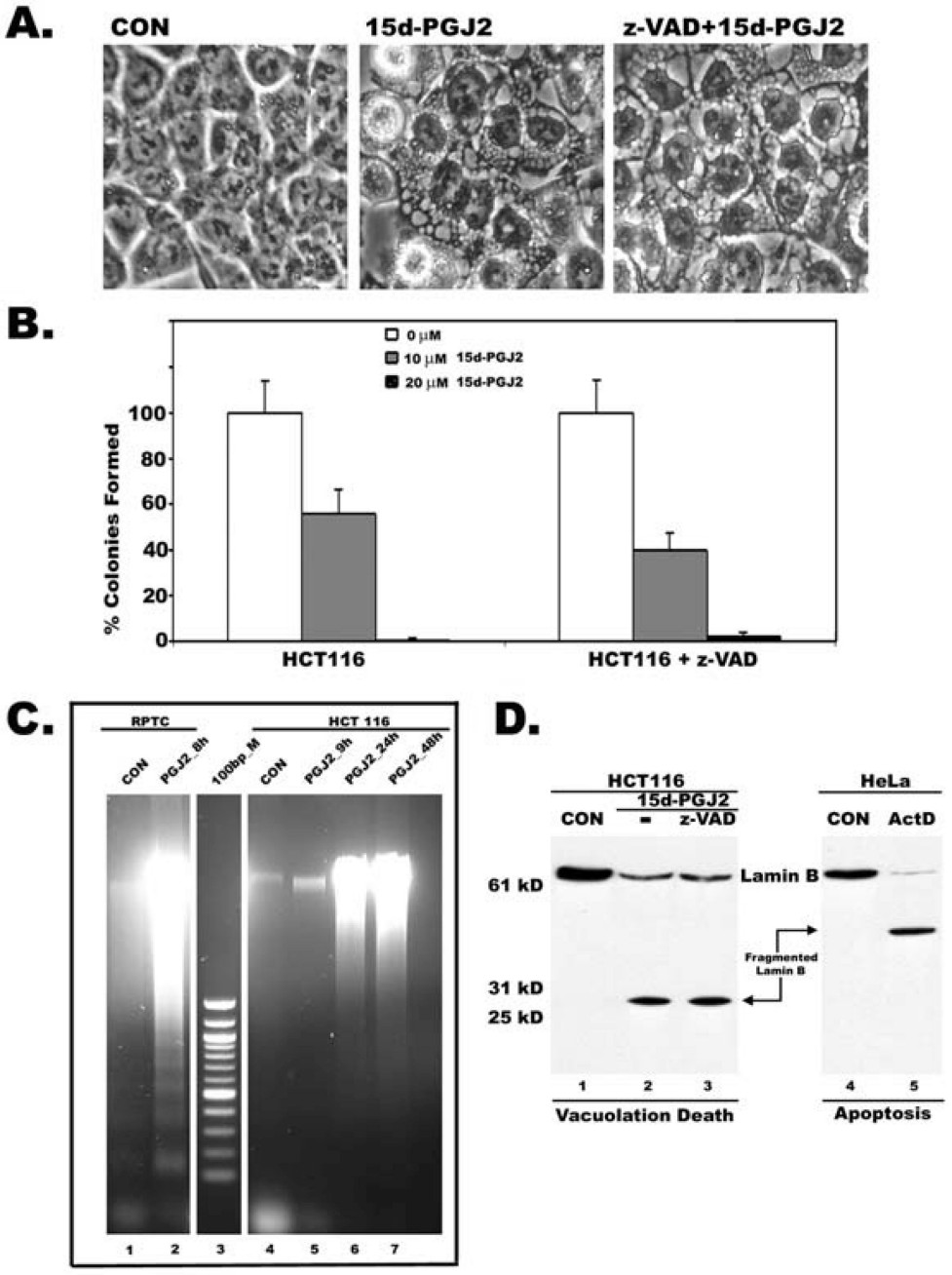

Figure 2. Cytoplasmic vacuolation death is associated with non-apoptotic and caspase-independent cleavage of Lamin B

A. Phase contrast image showing that broad-specific inhibitor of caspases, z-VAD, had no effect on 15d-PGJ2 induced cytoplasmic vacuolation. B. Decreased cell viability of HCT116 cells as assessed by clonogenic assay in the presence of z-VAD (50 μM) and 10 or 20 μM 15d-PGJ2. C. DNA from HCT116 cells treated with 15d-PGJ2 for 9h and shifted to normal medium for 24 and 48h 15d-PGJ2 show diffused pattern compared to DNA fragmentation of apoptotic rat kidney proximal tubule cells (RPTC); DNA samples were separated by agarose gel electrophoresis. D. Cell death was assessed by nuclear lamin B breakdown. Total lysates

from HCT116 cells treated with 15d-PGJ2 in the presence or absence of z-VAD and Hela cells treated with Actinomycin D (Act D) were compared by immunoblotting using a polyclonal antibody to lamin B.

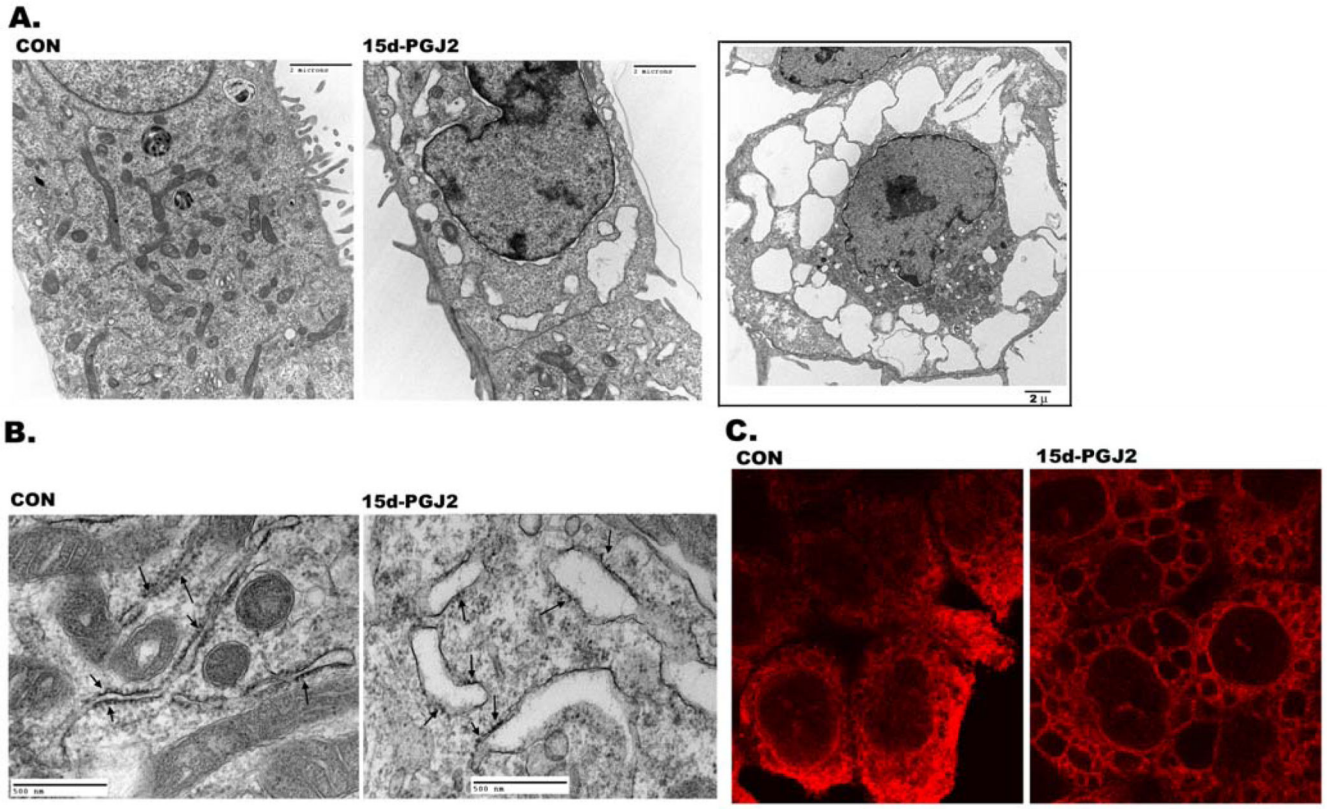

Figure 3. Dilatation of endoplasmic reticulum cisternae by 15d-PGJ2

Control and experimental cells were fixed after 15d-PGJ2 treatment and processed for electron microscopy as described in Experimental section. A. Transmission electron micrograph of untreated (control) and 15d-PGJ2 (20 μM) treated HCT116 cells for 6h. Inset shows cell with larger vacuoles after 9h treatment with 15d-PGJ2. B. Transmission electron micrograph of untreated (control) and treated (15d-PGJ2) HCT116 cells at higher magnification showing dilation of rough endoplasmic reticulum. Ribosomes are indicated by arrows. C. Confocal images of HCT116 cells immunostained for Calreticulin (red) without (CON) or with 15d-PGJ2 treatment. Cells were fixed after treatment and processed for immunofluorescence as described in Experimental section.

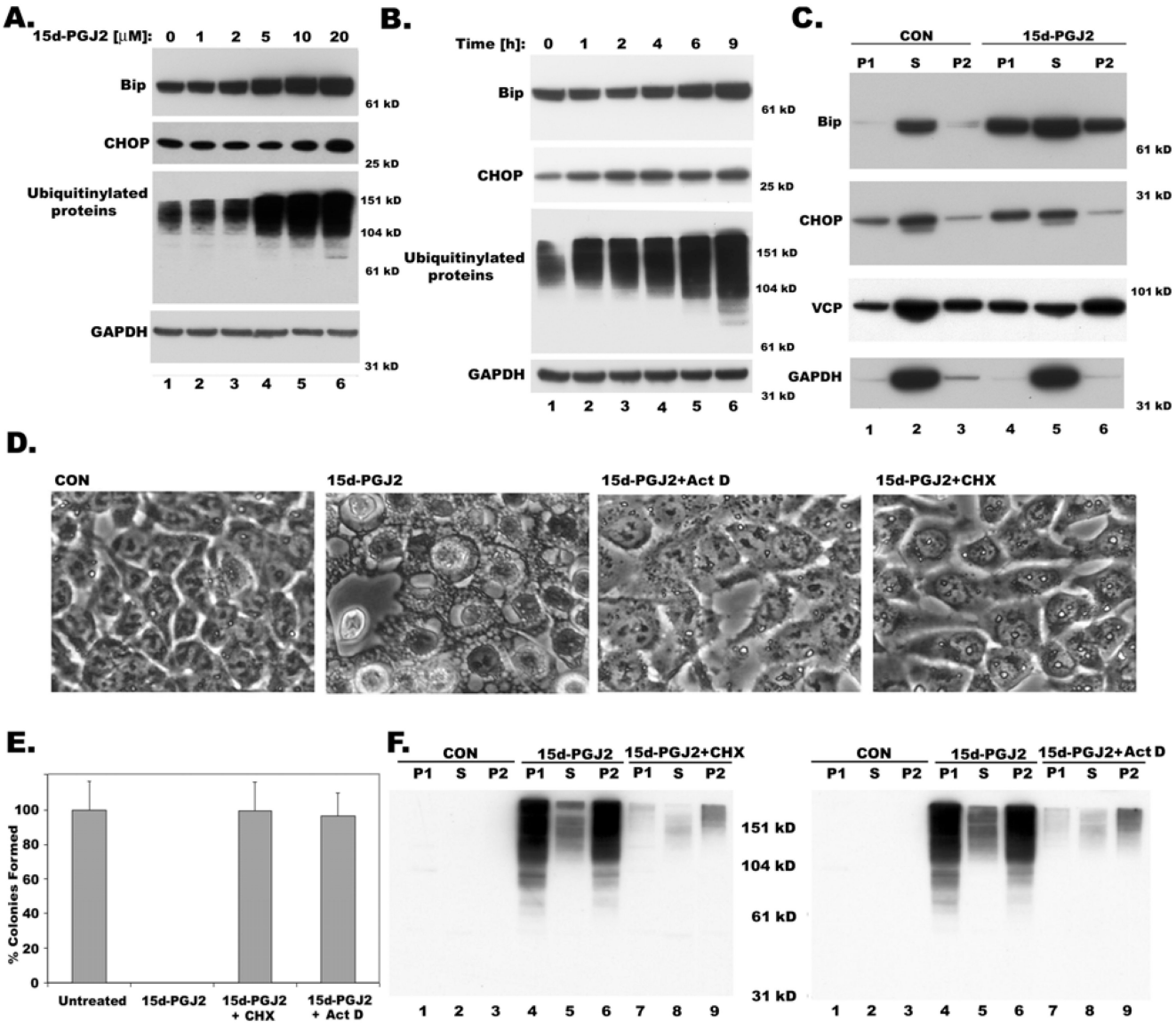

Figure 4. Dose and Time dependent expression of Bip and CHOP, ER stress markers and accumulation of ubiquitinated proteins in 15d-PGJ2 treated cells showing cytoplasmic vacuolation

A. Western blot showing expression of ER stress markers, Bip, CHOP and ubiquitinated proteins upon treatment with indicated doses of 15d-PGJ2 for 9h. B. Time course expression of Bip, CHOP and ubiquitinated proteins with 20μM of 15d-PGJ2 by western blotting at indicated hours. GAPDH is used as a loading control. C. Distribution of Bip, CHOP, VCP and GAPDH in detergent soluble (S) and insoluble low (P1) and high (P2) speed pellet fractions with or without 15d-PGJ2 treatment (20 μM) for 9h. Effect of transcription inhibitor, actinomycin D (20 μg/ml) and translation inhibitor, cycloheximide (25 μM) on cytoplasmic vacuolation induced by15d-PGJ2. D. Phase contrast images E. Cell viability as measured by clonogenic assay. F. Inhibition of accumulation of ubiquitinated proteins in

detergent insoluble fractions P1 and P2 by act D and CHX as shown by western blotting with ubiquitin antibodies.

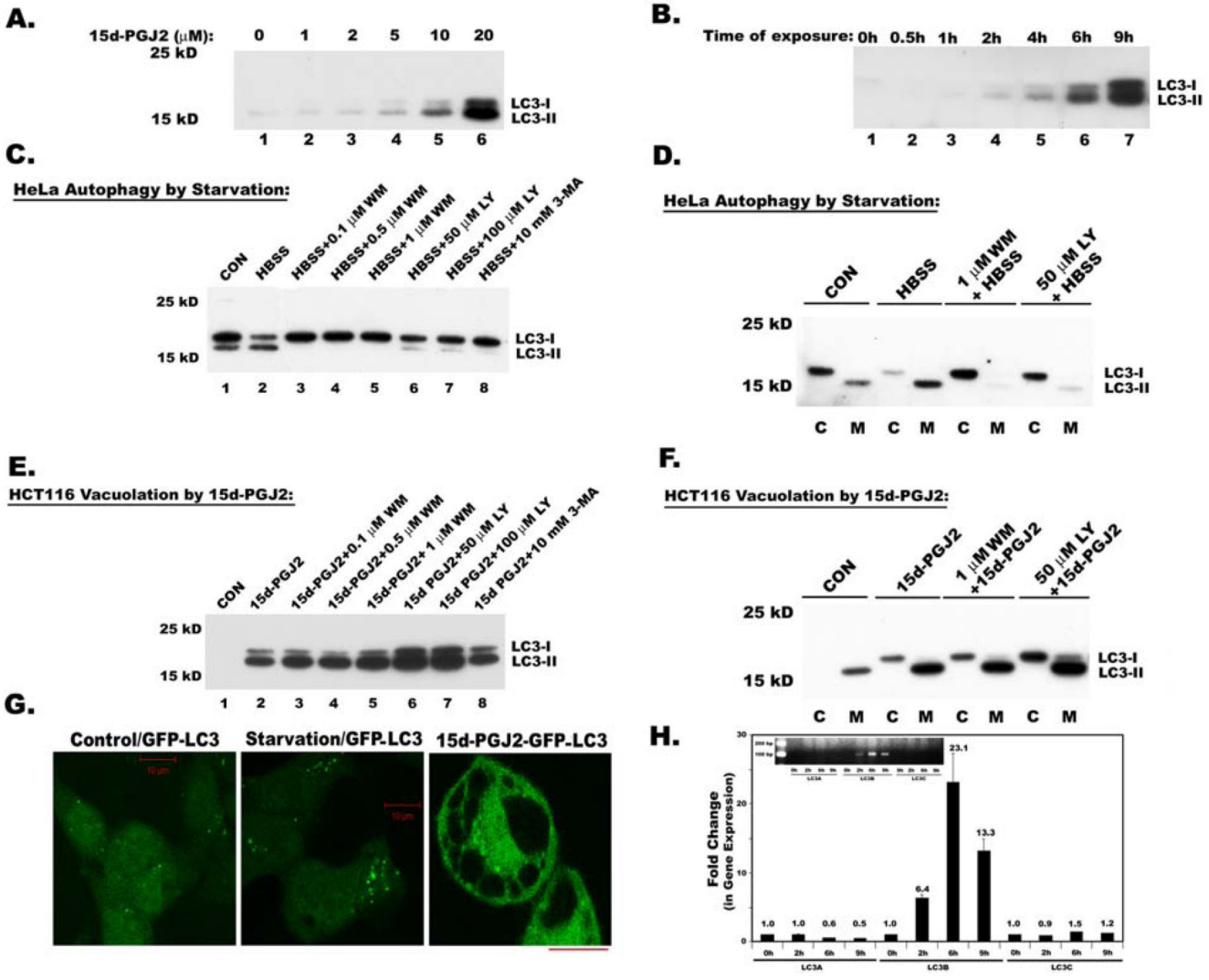

Figure 5. Expression and processing of autophagy marker, Map1 LC3 in serum starved HeLa cells and 15d-PGJ2 treated HCT116 cells

Total cell lysates were analyzed for Map1 LC3 (LC3) expression by immunoblotting A. Immunoblot analysis of dose dependent expression of LC3 in 15d-PGJ2 treated HCT116 cells at different doses for 9h. B. Immunoblot analysis of time dependent expression of LC3 in HCT116 cells after treating with 20 μM of 15d-PGJ2. C. Immunoblot analysis of LC3 in whole cell lysates of HeLa cells that were serum starved to induce autophagic processing of LC3. Effect of PI3-Kinase inhibitors LY294002 (LY), Wortmannin (WM) and 3 Methyl-adenine (3-MA) on starvation induced LC3 processing. D. Immunoblot analysis of LC3 in cytosolic (C) and membrane (M) fractions of Hela cells and effect of PI3Kinase inhibitors. E. Immunoblot analysis of LC3 in whole cell lysates during 15d-PGJ2 induced cytoplasmic vacuolation and effect of PI3-Kinase inhibitors LY294002 (LY), Wortmannin (WM) and 3 Methyl-adenine (3-MA) on 15d-PGJ2 induced LC3 expression and processing. F. Immunoblot analysis of LC3 in cytosolic (C) and membrane (M) fractions of 15d-PGJ2 treated HCT116 cells and effect of PI3K inhibitors. G. HCT116 cells that are constitutively

expressing GFP-LC3 were exposed to starvation or 15d-PGJ2 and were analyzed by confocal microscopy. The bar in these diagrams indicates 10 μ length. H. Quantitative real time PCR to analyze the expression of three isoforms of MAP1 LC3 using primers described in the Materials and Methods section. Insert shows relative expression of LC3 isoforms analyzed by agarose gel electrophoresis after 17 cycles of RT-PCR.

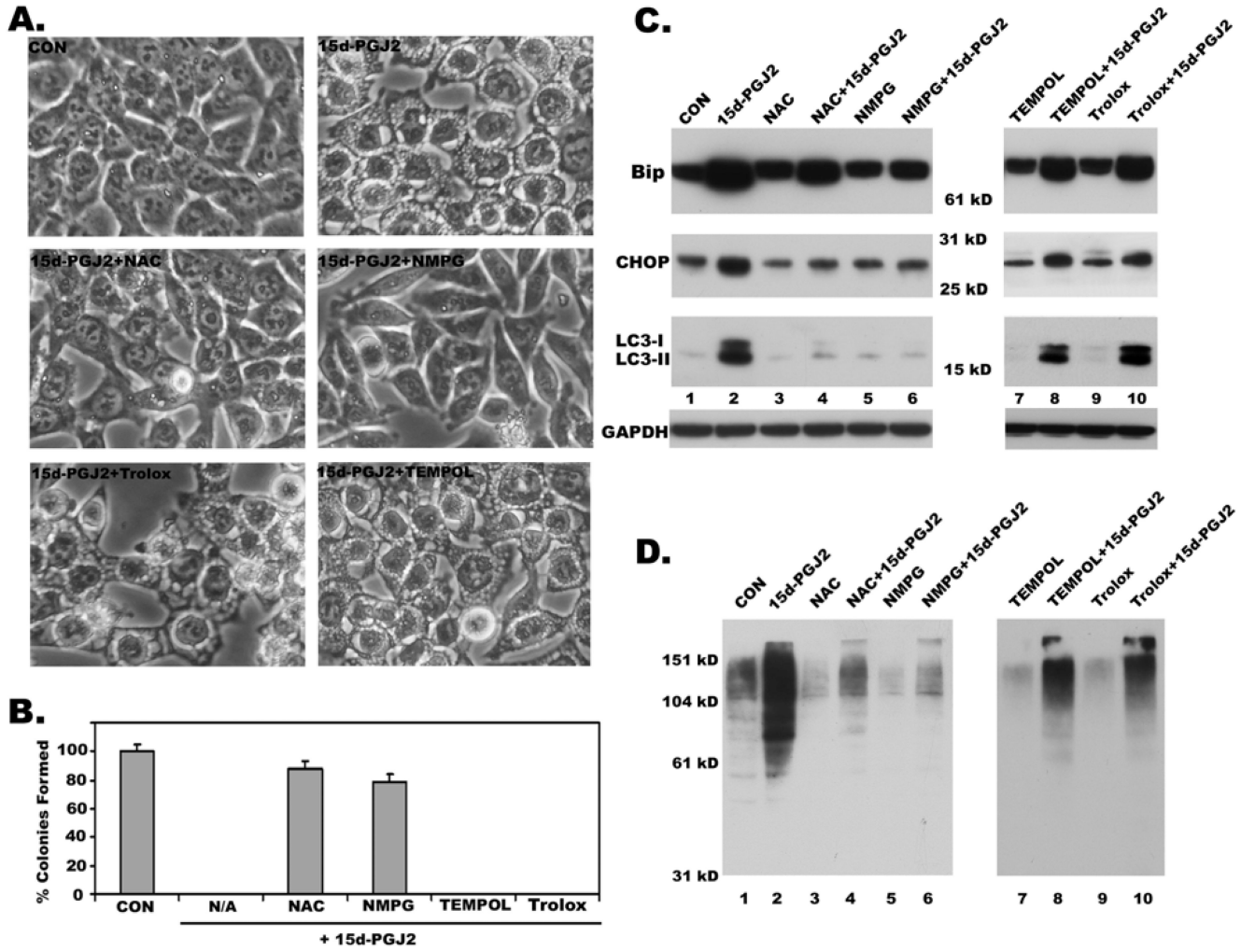

Figure 6. Effect of ROS scavengers on 15d-PGJ2 induced cytoplasmic vacuolation, cell death, ER stress and LC3 induction and processing

A. Effect of ROS scavengers, NAC, NMPG, TEMPOL and Trolox on 15d-PGJ2 induced cytoplasmic vacuolation as revealed by phase contrast images. B. Effect of ROS scavengers on cytotoxic effects of 15d-PGJ2 as measured by clonogenic assay. C. Immunoblots showing the effect of NAC, NMPG, TEMPOL and Trolox on the expression of ER stress markers Bip, Chop and processing and induction of LC3. D. Effect of above ROS scavengers on the accumulation of ubiquitinated proteins as revealed by western blotting with anti-ubiquitin antibody.

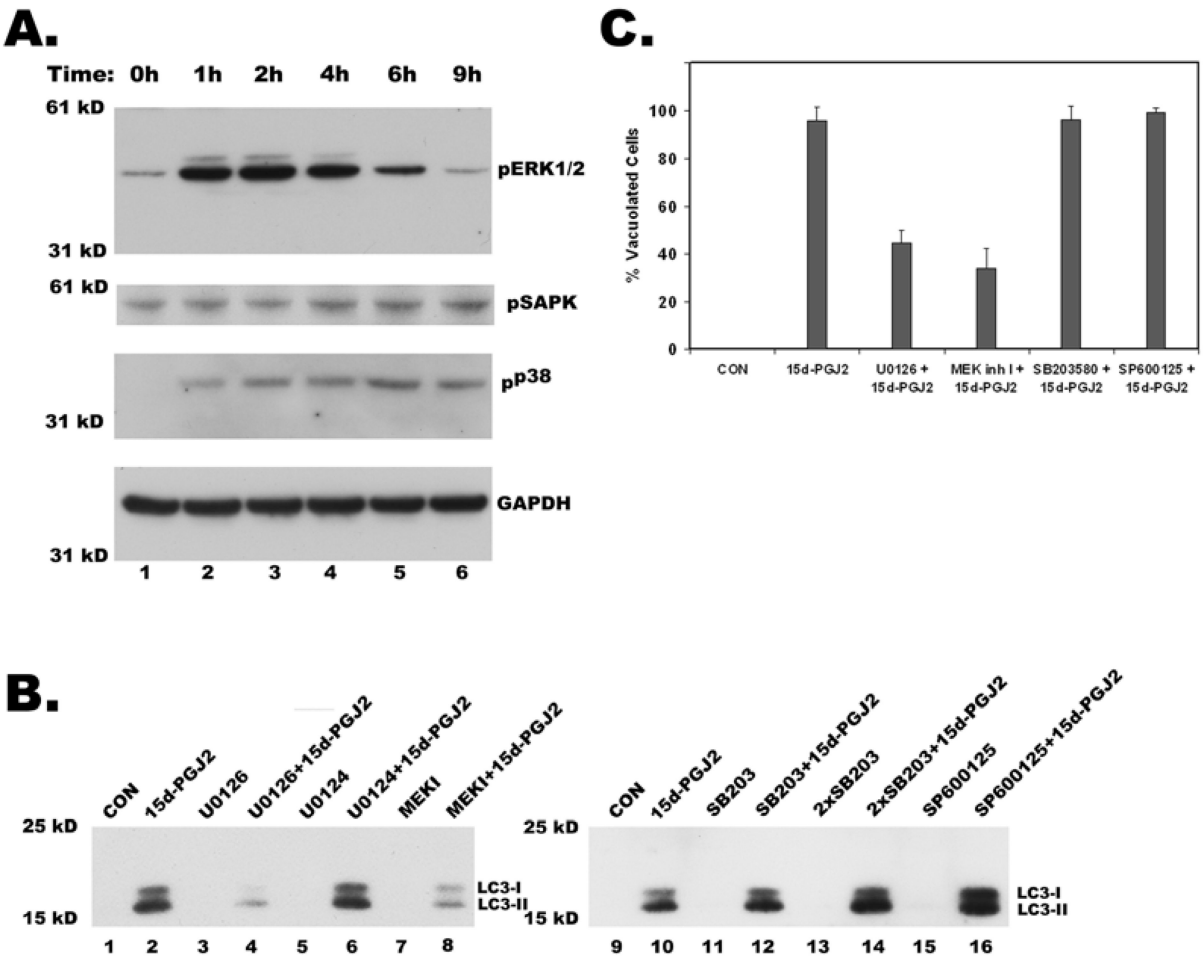

Figure 7. Regulation of 15d-PGJ2 induced cytoplasmic vacuolation, LC3 expression and processing by MAP kinases

A. Western blot of total cell lysates showing activation of MAP kinases ERK, p38 and JNK (SAPK) upon treatment with 20μM 15d-PGJ2 at indicated times in hours. Activation of MAP kinases was shown by immunoblotting with their phospho-specific antibodies. B. Effect of U0126 (20 μM), and MEK inhibitor I (MEK I, 5 μM), specific inhibitors of ERK pathway, U0124 (20 μM), an inactive analog of U0126, SB203580 (SB203) at 10 μM and 20 μM (2X), inhibitor of P38 MAP kinase and SP600125 (20 μM), JNK pathway inhibitor on 15d-PGJ2 induced expression and processing of LC3. After 1h of preincubation with the above inhibitors, cells were treated with 15d-PGJ2 for 9h and then were probed for LC3 by western blotting of total cell lysates. C. Effect of MAP kinase inhibitors on 15d-PGJ2 induced cytoplasmic vacuolation. Cells were treated as described above, phase contrast images were obtained from different fields and number of vacuolated cells was counted in at least 100 cells for each condition and data represents an average of three independent experiments.

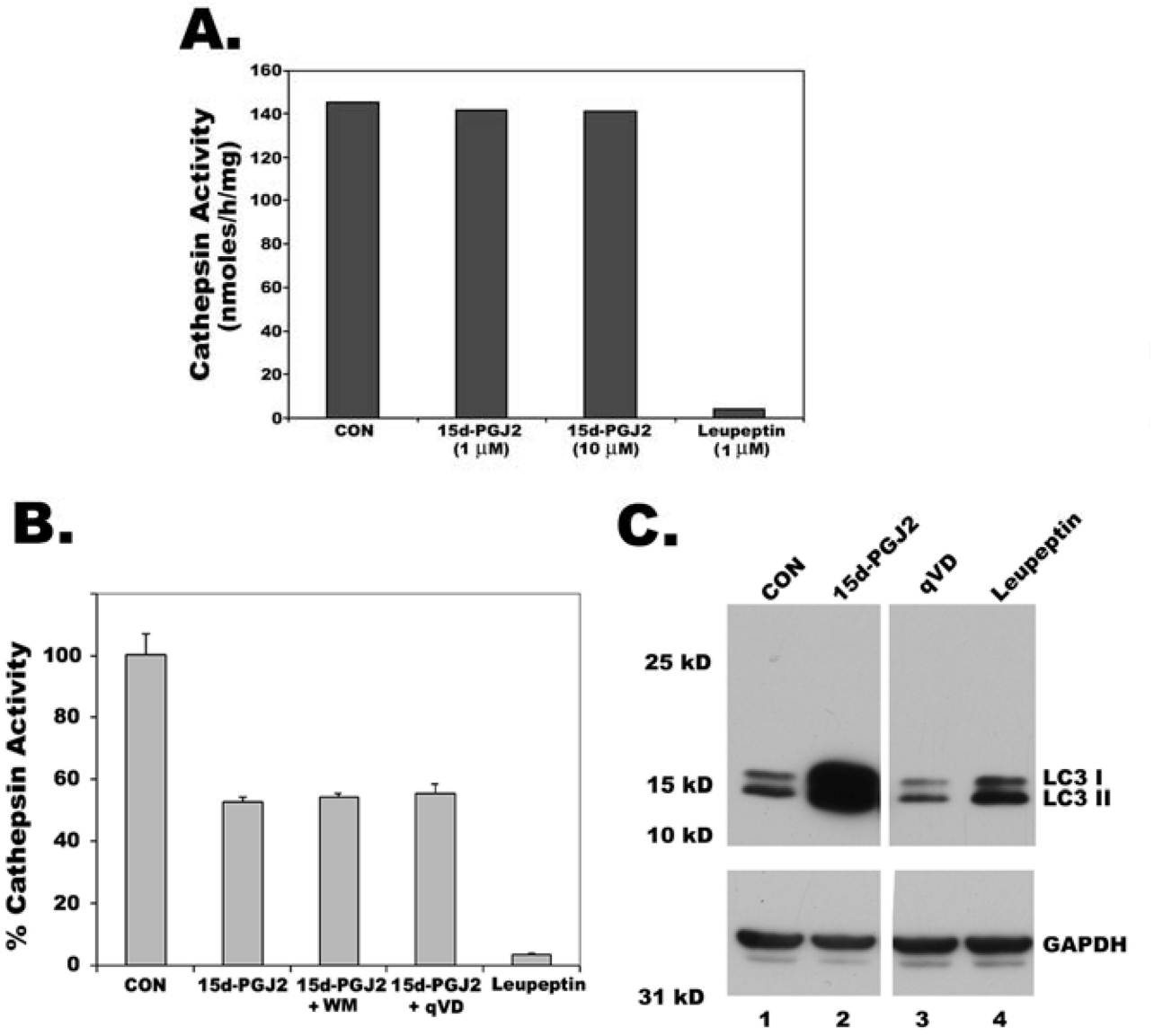

Figure 8. Increase of LC3 by 15d-PGJ2 is not through inhibition of lysosomal protease activity

A. Cathepsin L activity in untreated HCT116 cell extracts was measured through hydrolysis of Z-Phe-Arg-AMC as described in materials and methods section. Extracts were preincubated with either 15d-PGJ2 or leupeptin before measuring the activity. B. Cells were treated with either leupeptin, or 15d-PGJ2 or 15d-PGJ2 with Wortmannin (WM), an autophagy inhibitor or 15d-PGJ2 with caspase inhibitor q-VD for 9h. Membrane bound fractions were collected and assayed for Cathepsin L activity. C. LC3 expression in HCT116 cells treated for 9h with either cathepsin inhibitor, leupeptin or 15d-PGJ2 or caspase inhibitor, qVD was analyzed by immunoblotting.

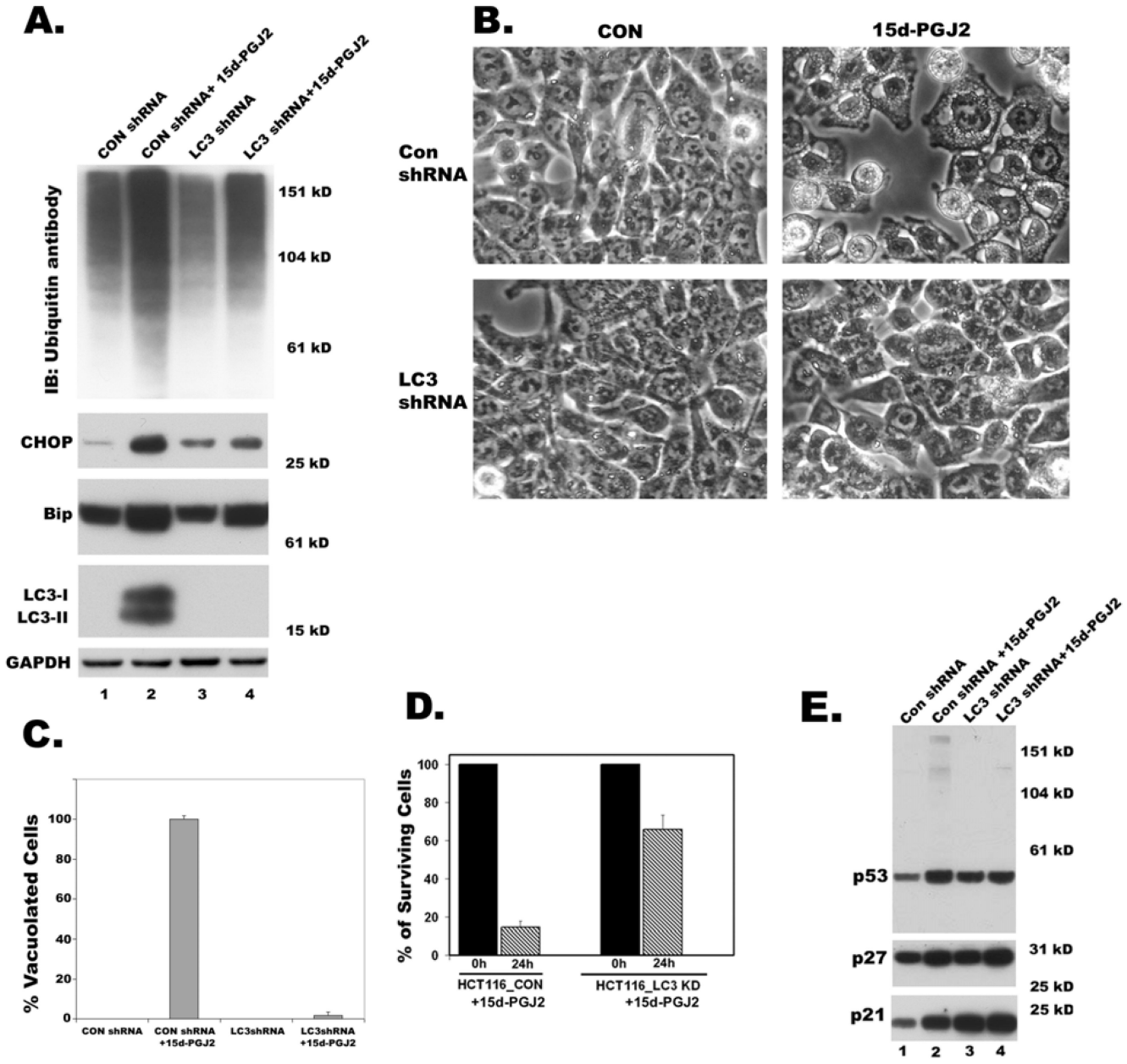

Figure 9. Effect of LC3 knockdown on 15d-PGJ2 induced cytoplasmic vacuolation and cell death

Clones of HCT116 cells expressing GFPshRNA (CONshRNA) or LC3 shRNA were obtained. A. Western blots of total cell lysates showing the effect of knockdown of LC3 on 15d-PGJ2 induced accumulation of ubiquitinated proteins, expression of ER stress markers, Bip and CHOP and expression and processing of LC3. B. Phase contrast images showing effect of LC3 knockdown on 15d-PGJ2 induced cytoplasmic vacuolation. C. Bar graph showing percentage of vacuolated HCT116 cells that were expressing CONshRNA or LC3 shRNA with or without 15d-PGJ2 treatment. D. Cell viability determined by trypan blue exclusion assay after growing clones of HCT116 cells for 24h in growth medium after incubating with 15d-PGJ2 (20 μM) for 9h. Data represents an average of three independent

experiments. E. Western blots of total cell lysates showing effect of LC3 knockdown on 15d-PGJ2 induced expression of p53, p21, p27 in HCT116 cells.